Roof-Shaped Clathrate Compounds as Novel Coating Materials for the Detection of Organic Solvent Vapours: A Study Focussed on Thickness Shear Mode Resonators as Mass-Sensitive Transducers

J. Reinbold and K. Cammann*

Münster, Westfälische Wilhelms-Universität, Anorganisch-Chemisches Institut, Lehrstuhl für Analytische Chemie

E. Weber, T. Hens, and C. Reutel

Freiberg, Technische Universität Bergakademie, Institut für Organische Chemie

Received January 22nd, 1999

Dedicated to Prof. Dr. Fritz Vögtle on the Occasion of his 60th Birthday

Keywords: Mass-sensitive device, Thickness shear mode resonator, Sensitive coatings, Inclusion compounds, Molecular recognition, Organic solvent vapour detection

Abstract. The performance of new crystalline inclusion hosts as chemical sensitive coatings for the detection of organic solvent vapours was investigated by using 10 MHz thickness shear mode resonators as mass-sensitive transducers. The crystalline host compounds under study consist of a characteristic 9,10-dihydro-9,10-ethanoanthracene framework with appended diarylmethanol clathratogenic groups **1**, **2** or an analogous subunit **3**. Relating to the selectivity of inclusion formation a database was generated consisting of the calibrated sensor responses from nine substituted versions of this host to each of seven organic solvent vapours (and humidity). From molecular shape, polarity and lipophilicity preferred inclusion selectivity was found for alcohol vapours, in particular for ethanol and methanol, thus indicating the predominant role of hydrogen bonding interaction. The inclusion of guest molecules with higher molar volumes was frequently accompanied by slow inclusion rate and sensor response, respectively. By decreasing the host size a general decrease of the sensor sensitivities were observed, but the selectivity (sensitivity pattern) is shifted to smaller molecules, and inclusion is widely controlled by kinetic parameters. By time-dependent data acquisition improved selectivity for analyte molecules with fast inclusion kinetics was obtained, especially for methanol vapours. Moreover, the long-time stability of the coatings was evaluated showing excellent (mass) stability, even over a period of more than two years.

The development of receptor-based chemical sensors for gas sensing, and in particular for monitoring volatile organic compounds (VOCs) is widely determined by the sensitive properties of the coating material. Therefore, the design and characterization of new chemically sensitive materials continues to be an active area of research [1, 2]. Mass-sensitive devices such as the quartz microbalance (QMB) are versatile devices to study the sensor characteristics of different coating materials, such as polymers [3–5], supramolecular compounds for mono- [6–9] and multimolecular inclusion [10–12], thin self-assembled films [13], liquid crystals [14] or coordinating compounds [15].

With reference to the QMB its main component is the piezoelectric quartz crystal as mass-sensitive transducer, usually a temperature compensated cut (AT) derived from a quartz single crystal, as it is mass-manufactured for electronic applications [16, 17]. For gas sensing applications the quartz crystal is an external component of an oscillator circuit operating in its fundamental thickness shear mode at a frequency ranging from 1 MHz up to 30 MHz [18]. In view of their acoustic wave propagation these transducers are denoted as thickness shear mode resonators (TSMR). Frequently used TSMRs operate at a resonant frequency of 10 MHz (quartz plate thickness 168 µm).

First theoretical investigations of mass-frequency relation was carried out by Sauerbrey, who derived a linear relationship between the frequency and small added masses onto the active area of the TSMR [19, 20]:

$$\Delta f = - C \cdot \Delta m / A \quad \text{with} \quad C = 2 f_0^2 / (\rho v) \tag{1}$$

with the frequency shift Δf (in Hertz), and $\Delta m/A$ the surface mass loading in grams per square centimetre. The constant C is defined as the mass sensitivity or calibration constant and relates to the fundamental frequency f_0 in Hertz, and two material constants of the quartz crystal (density ρ = 2,650 g/cm^3, share wave velocity u = 334 000 cm/s). The Sauerbrey equation is valid up to mass changes of 2% of the whole plate mass and the frequency shift, respectively.

For the 10 MHz TSMRs used in this study (C = 2,26 10^8 cm^2 Hz^{-1} g^{-1}; A = 0,25 cm^2) average shifts due

  1436-9966/99/3410X-252 $ 17.50 + .50/0

to coatings (Δf_{coat}) are in the 25 kHz range, resulting from a deposited mass of approximately 28 µg, which corresponds to an average film thickness (t_{coat}) of ≈ 1,1 µm, assuming unit density for the coating material.

The response of the coated transducer to a vapour compound (Δf_{vap}) depends on the degree of equilibrium partitioning between chemical coating and gas phase, which in turn depends on the amount of coating deposited on the transducer. Due to medium vapour concentrations usually a linear signal-to-concentration-sensitivity is observed which, on the other hand, increases linearly with Δf_{coat}. It can be assumed that the mass loading effect is predominant, whereby the partition coefficient K can be calculated from measured data according to the following equation

$$K = c_{coat} / c_{vap} \qquad \text{with} \qquad K = \frac{\Delta f_{vap}\, \rho_{coat}}{\Delta f_{coat}\, c_{vap}} \qquad (2)$$

where c_{vap} denotes the vapour concentration and ρ_{coat} the coating density, both to be used with the same units, *e.g.* grams per liter. To estimate the sensor response several semi-empirical models describing the equilibrium vapour-coating solubility have been developed, being deduced from gas-liquid-chromatography (GLC) [21, 22]. Initially these models were mainly applied to amorphous polymer coatings and have recently been extended to supramolecular compounds [23]. In this context the structure-related term "molecular recognition" is discussed controversially [23, 24]. For solid coatings the equilibrium partitioning is predominantly determined by adsorption and for the calculation of K the coating density is not considered, so that K is finally expressed as K_c with the dimension volume per mass (frequently given in the units liter per grams [23]).

The aim of this study is to investigate potential effects such as hydrogen bond interaction and solubility of the enclathrated molecules on the sensitivity patterns of the clathrate host coatings. Moreover, it is intended to find out whether the selectivity can be improved by analysing the time dependence of the sensor response.

Experimental

Materials

The host compounds **1a**–**d**, **2a**–**d** and **3** (Scheme 1) were prepared as described elsewhere [25, 26].

For the generation of the calibration vapours organic solvents (Merck, Darmstadt and Fluka, Neu-Ulm, Germany) of chemical "pro analysi" grade (> 99% pure) were used, without further purification. Humidity atmospheres were prepared with deionized water having impurities less than 0,1 µS/cm. Carrier and dilution gas for all vapours was dry synthetic air with a purification grade of 5.0 (≥ 99,999%).

Transducers and Coatings

For transducer preparation, quartz crystals (AT-cut) with circular deposited silver electrodes were used, operating at a fundamental frequency of 10 MHz. The quartz crystals (fabricated by International Quartz Devices; Somerset, England) were purchased from Farnell Electronic Components (Deisenhofen, Germany). On delivery they are already fixed on HC-18-sockets, with the advantage of stress-free holding and compatibility to standard connectors. After removal of the housing cap the quartz crystals were rinsed with isopropanol and dried in an inert gas stream (N_2) to eliminate possible contaminations. For the coating procedure a solution of approximately 2,5% (m/m) of **1a**–**d**, **2a**–**d** and **3**, respectively, was prepared in tetrahydrofuran and deposited onto both sides of the active surface by drop coating technique employing a micropipette with terminal teflon stamp. The initially rough films were homogenized by a short incubation of the coated transducer in a saturated ethanol atmosphere. Well-adherent coating layers with smooth surface were obtained, as it is shown in Fig. 1 (right).

In all cases, the total shift in frequency was observed. The following TSMRs were fabricated.

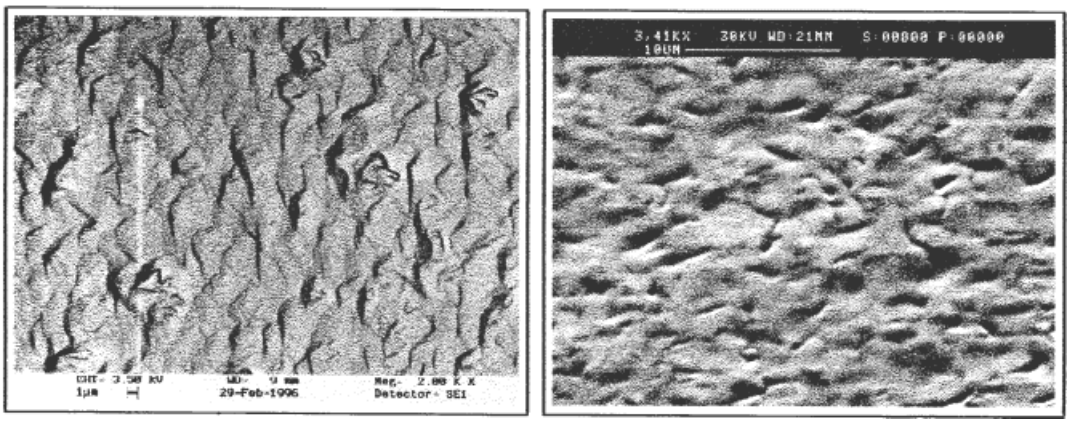

Fig. 1 Scanning electron microscopy image of a section of (left) an uncoated silver electrode (zoom-in 2000-fold) to which the inclusion compound **1c** (29,95 kHz) has been applied by drop coating, and (right) after homogenization (zoom-in 3410-fold).

Table 1 Survey of the coated 10 MHz TSMR including host compounds **1a**–**d**, **2a**–**d** and **3**

Coating	**1a**	**1b**	**1c**	**1d**	**2a**
Δf_{coat} (kHz)	45,70 ± 0,05	51,93 ± 0,06	29,95 ± 0,05	18,51 ± 0,04	30,68 ± 0,06
t_{coat} (μm)	1,69 ± 0,17	1,87 ± 0,19	1,08 ± 0,11	0,62 ± 0,06	1,14 ± 0,11
Coating	**2b**	**2c**	**2c**	**2d**	**3**
Δf_{coat} (kHz)	45,60 ± 0,19	9,87 ± 0,03	20,90 ± 0,05	22,12 ± 0,03	23,11 ± 0,08
t_{coat} (μm)	0,794 ± 0,08	0,36 ± 0,04	0,75 ± 0,08	0,74 ± 0,07	0,79 ± 0,08

The Δf_{coat} values in Table 1 represent average data from the recorded baselines of every measurement corresponding to the first purging level with dry air. The obtained standard deviations indicate stable coating layers and reproducible experimental conditions. The exact Δf_{coat} values are given below. To estimate the film thickness t_{coat} the mass term in equation 1 was substituted by the density of the coating material, resulting in an equation to calculate the film height. If possible, the densities of the free host compounds were taken from the literature [25–28]. It has to be noted, that some of the densities relate to the inclusion compounds, but differ slightly to that of the free host [26]. Due to an error propagation from the calculating method, an experimental error of approximately 10% was assumed owing to the deviation of the coating density, the deviation of Δf_{coat} and a homogenous coverage of the film, respectively.

Instrumentation

The complete experimental setup consists of the following units: (i) an equipment for producing and diluting calibration gas mixtures, (ii) a multiplex-controlled four-channel-quartz microbalance, both designed in our laboratory. Controlling functions as well as data acquisition, calculation and visualisation are performed by a self-developed computer software, for both the sensor device and the gas calibration system.

Sensor Device and Data Acquisition

The multiplex-controlled four-channel sensor device comprises a gas measuring chamber, with four coated TSMRs and one uncoated reference TSMR. Each quartz crystal is powered by a modified Colpitts series resonance oscillator, placed separately in the electronic unit close to the measuring chamber (Fig. 2). The temperature of the complete device was maintained at (296 ± 0,1) K by a microprocessor-controlled thermostat (Haake C25/F6; Haake, Karlsruhe, Germany), precision ± 0,02 K. The thermostated water circulated through the channels in the aluminium housing (10 cm × 10 cm × 6 cm). The actual temperature was monitored by a Pt-100 resistance thermometer placed near the sensors.

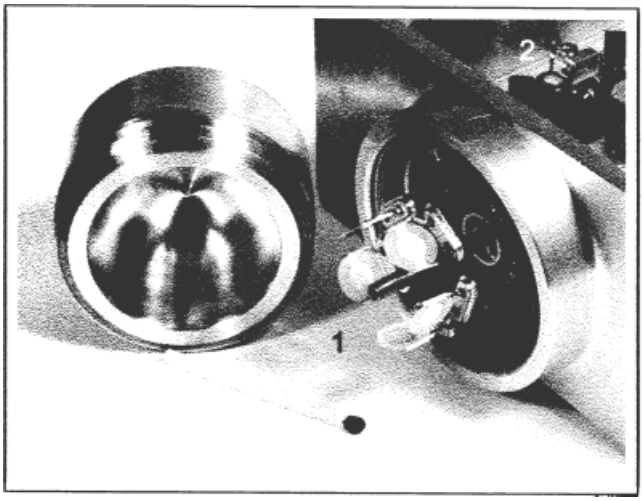

Fig. 2 Sensor device comprising the TSMR arrangement in the opened gas cell (1) and the oscillator electronic unit (2).

The TSMR outputs were connected to a signal processing unit. Its operating principle is presented in Fig. 3. To obtain the four low-frequency difference signals between each sample quartz and the reference quartz, the original frequencies were amplified, mixed by four double-balanced mixers and band-pass filtered. After scaling by Schmitt-triggers the signals were fed to the multiplexer, transferring each signal to the frequency counter (Hewlett Packard 53131a). This frequency counter was provided with an internal oven-stable time base, allowing for high signal resolution (10 digits/s) and thus for a satisfying sampling rate during multiplex operation. Sensor data were sampled with 0,25 Hz per channel at 0,002 Hz resolution (gate time: 300 ms) and logged to the personal computer *via* RS 232.

Sensor Response and Signal Analysis

The sensor responses are given by the signal height resulting from the frequency difference between the given gas exposure and the purging level. This is denoted as the sensor mode. Occasionally, for coating layers with high sensitivity but slow inclusion kinetics the equilibrium state was not reached during the exposure period. In such cases the curve data were fitted by a Boltzman function and data were extrapolated according to the equilibrium state. The relative error of the fitted data is assumed to 10% , indicated by error bars. It must be emphasized that all response curves shown in the Result Section relate to the measured raw data obtained from the frequency counter, and are presented without any modification such as averaging, drift compensation, *etc*. The original frequency value is given at the left ordinate, and the net signal is shown at the right ordinate, respectively. To show kinetic inclusion characteristics, the first derivative of the frequency signal was calculated, and the signal height as the reversal point of the sensor curve was evaluated. In this mode only concentration changes can be recorded, according to a detector operation. Partition coefficients K_c [l/g] were calculated from equation 2, where the density of the coating is not considered (see Introduction). To characterize the sensor quality, the shift of baseline was recorded over the measuring period by taking some data points at the end of every purging

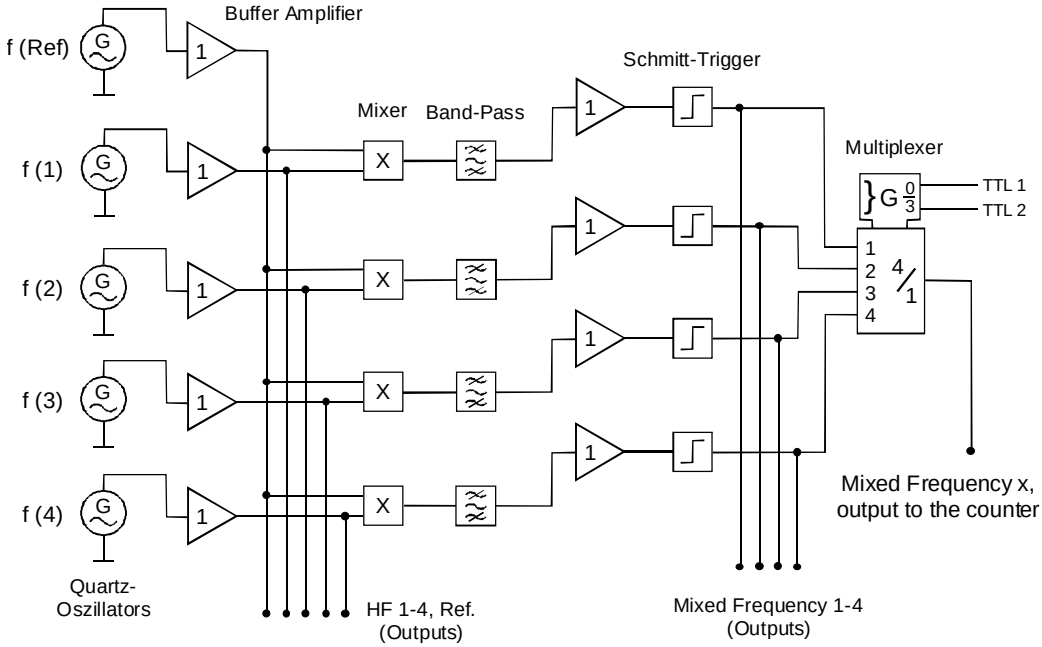

Fig. 3 Block diagram of the radio frequency (rf) electronics and signal processing.

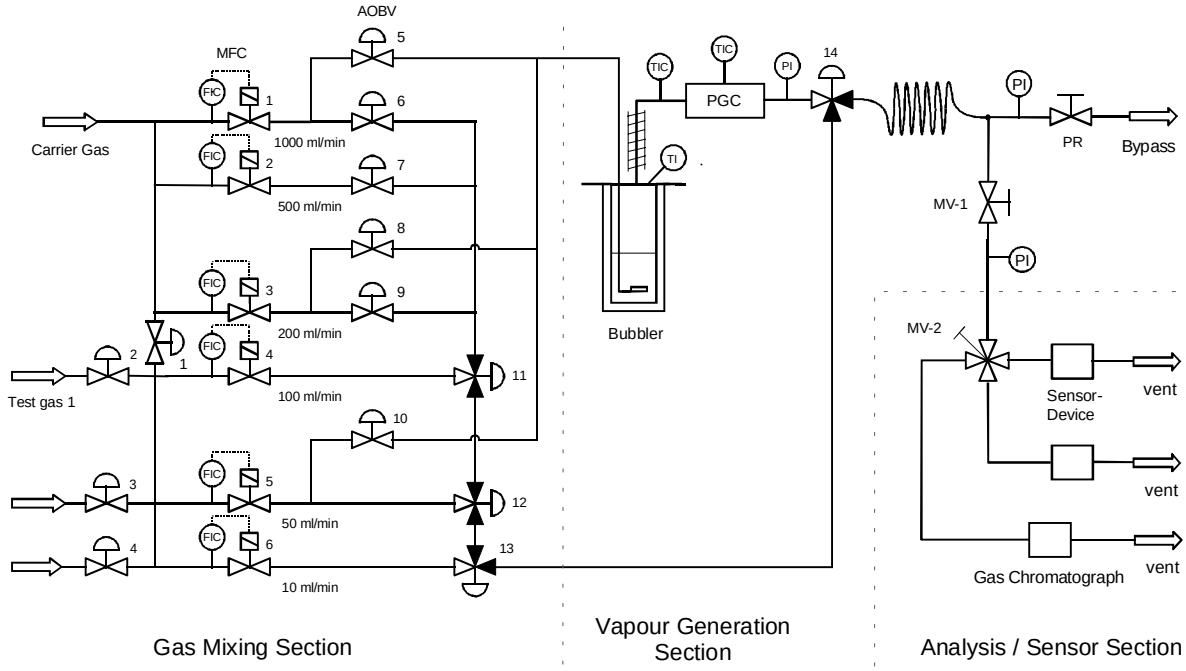

Fig. 4 Dynamic test gas generation system. MFC: mass flow controller; AOBV: air operated bellows valve; PGC: peltier gas cooler; TI: temperature instrument; TIC: temperature instrument controller; PI: pressure instrument; MV: mechanical valve; PR: pressure reducer.

period, directly before a new vapour exposure. The quotient of the baseline signal difference at the start time and the end of the measuring period was used to calculate an average drift level per hour. The noise of the sensor signal is given by the standard deviation calculated from approximately 100 data points of the baseline, and the limits of detection (LOD) were estimated corresponding to a signal-to-noise ratio of 10.

Vapour Generation and Gas Mixing System

Vapour calibration gases were dynamically generated by the saturation method according to the VDI-guideline 3490 [29]. The flowchart of the experimental setup is shown in Fig. 4.

Defined vapour atmospheres were produced by passing a continuous carrier gas flow from the mass flow controllers (MFC; MKS Instruments) ## 1, 3, or 5 through the fritted

bubbler containing the liquid solvent at room temperature. The obtained gas mixture was then cooled in a peltier element-driven condenser (precision ± 0,02 °C), where the excess fraction of the solvent condensed. The resulting vapour pressure of the solvent at cooling temperature was calculated using the semi-empirical Antoine equation, where the volume fraction of the component is given by the ratio of its vapour pressure to the total pressure. To set the desired concentration, the component gas flow was diluted with the appropriate carrier gas flow. All MFC except that one controlling the saturation flow can be used for dilution steps, provided that the air operated bellows valves are appropriately configured (Fig. 4). The concentrations of the generated vapours were verified semi-continuously by a gas chromatograph (Shimadzu, GC-17a) comprising a pneumatically driven six-port-two-position injection valve (Valco Instruments) for automated sample injection. After eluting the solvent from the column (HP-1: 5 m; 0,53 mm; 2,65 µm) its amount was quantified by a flame ionisation detector. The gas mixing setup operates linearly over a range of approximately three concentration decades with a random error less than 0,2%, where the minimum and the maximum concentrations depend on the vapour pressure of the solvent and the cooling temperature. To estimate the systematic error of this method, the results of the saturated vapour analyses were compared to those of certified standards (for ethanol and tetrachloroethene), showing an average deviation less than 5%. This is in good agreement with the estimated maximum relative error based on the determinable individual errors of the temperature and pressure measurement and of the vapour pressure calculation [29].

To estimate the vapour sensitive characteristics of the clathrate coatings, a representative selection of the following vapours was generated: water (humidity), methanol, ethanol, 1-propanol, toluene, tetrahydrofuran, and tetrachloroethene. Routine calibrations were made by purging with synthetic air for 10 min, followed by 5 min. periods of alternating exposure and purging. Concentrations vary from 1000 ppm, 2000 ppm to 3000 ppm (water, methanol), from 425 ppm, 1150 ppm to 2150 ppm (ethanol) and from 200 ppm, 600 ppm to 1000 ppm for the other organic solvent vapours. When slow sensor response was observed, the purge and exposure cycle period was extended two- or fourfold. A constant gas flow of 300 ml/min was fed from the bypass to the sensor device (Fig. 4).

Results and Discussion

As we have shown previously, crystalline host compounds, mostly of bulky difluorenol structure, have proved to be appropriate as sensitive coatings for the detection of organic solvent vapours [10 – 12]. Here, we report for the first time about the sensing characteristics of the roof-shaped solid hosts **1** – **3** with respect to selected volatile organic compounds and humidity using TSMRs as mass-sensitive transducers. Common to this particular type of host structures is a roof-shaped 9,10-dihydro-9,10-ethanoanthracene framework having diarylmethanol clathratogenic groups **1**, **2** or an analogous subunit **3** attached to it. The ability of these compounds to form clathrates mostly depends on intramolecular interactions, mainly on rather strong hydrogen bonds and on weak OH $\cdots\pi$ interactions. Numerous X-ray studies of inclusion compounds of **1** and **2** prepared by cocrystallization from solution have revealed that the host structures exhibit two predominant conformations (Fig. 5) [30].

Structure (a) in Fig. 5 is indicative of the so-called “active” conformation where the two OH-groups form a relatively strong intramolecular hydrogen bond. This conformation frequently occurs when the host includes polar guest molecules having pronounced proton donor and/or acceptor properties. In the other conformation (Fig. 5b) the OH-groups are directed towards the aryl rings of the dihydroanthracene moiety thus forming weak OH $\cdots\pi$ interactions. Here an eminent clathrate formation ability for aromatic hydrocarbon guests is observed [30]. Significantly different inclusion properties of these conformations are most likely due to the different guest recognition modes.

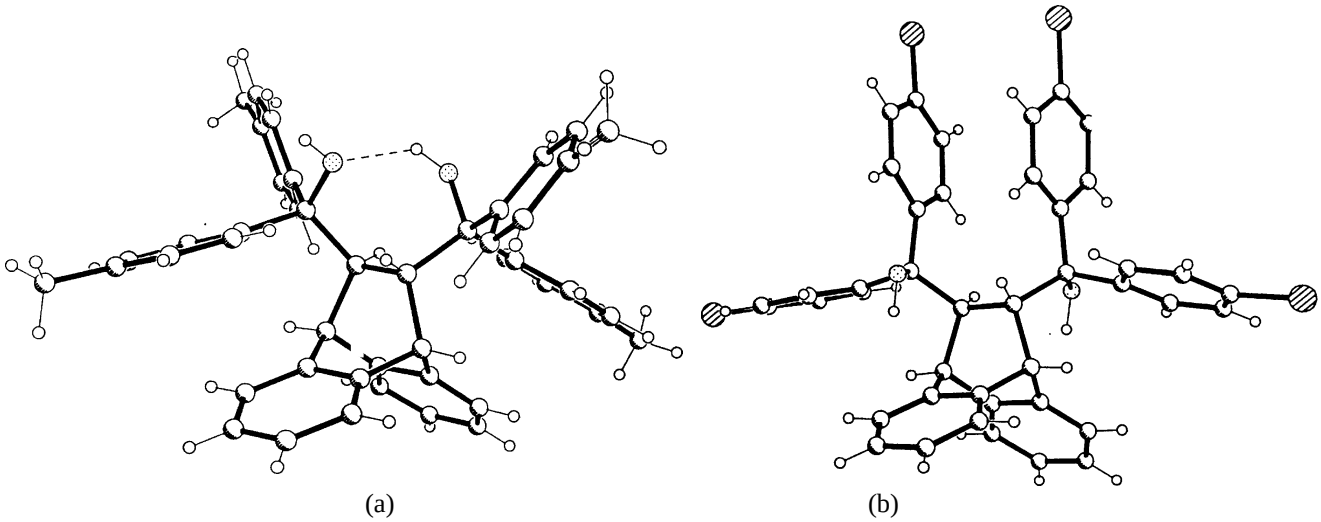

(a) (b)

Fig. 5 Perspective illustration of the ‚active‘ (a) and ‚inactive‘ (b) conformation shown by the present roof-shaped diol hosts **2**.

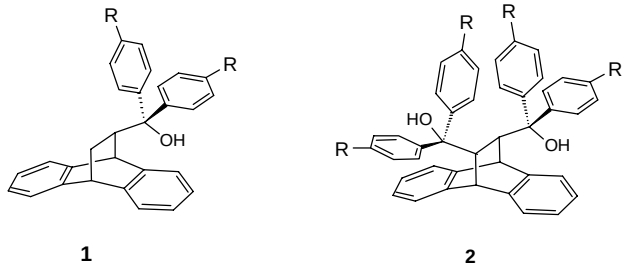

1 **2**

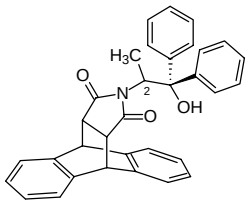

3 (2*RS*)

a: R = H
b: R = CH_3
c: R = $C(CH_3)_3$
d: R = Cl

Scheme 1

Sensor Responses and Detection Principles

Sensor measurements using coated quartz crystals are based on the sorptive inclusion mechanism. The inclusion formation is detected by the sensor response given by the frequency shift of the quartz crystal (Δf_{vap}). In contrast to the cocrystallisation experiments, thermodynamic and in particular kinetic aspects of the inclusion formation have to be considered here. In this context, some typical sensor characteristics of the inclusion compounds are introduced (cf. Fig. 6). For all tested coatings **1** and **2** we found satisfactory sensitivities to alcohols increasing from methanol to 1-propanol as expected. The remarkable feature of the inclusion of methanol, as the smallest alcohole molecule, is a short response time leading to a reversible sensor response with an excellent baseline stability. Typical time dependent sensor responses of the coating **2c** to various methanol and 1-propanol concentrations are shown in Fig. 6.

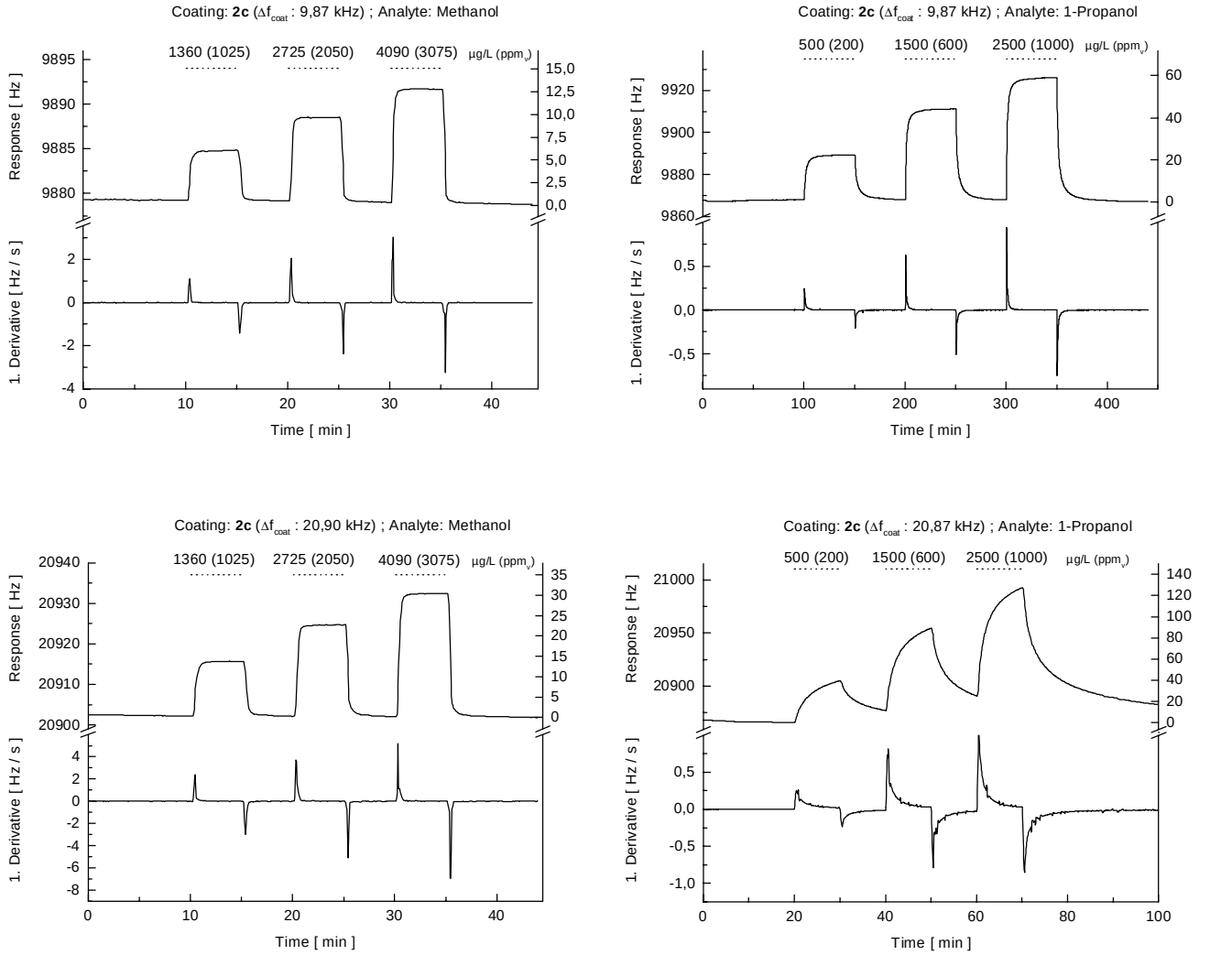

Fig. 6 Response of host compound **2c** to methanol and 1-propanol. Each plot represents two response curves: the original frequency data on top and its first derivative below. The two plots (top) result from the sensor **2c** (9.87 kHz) and the two plots (bottom) relate to the sensor **2c** (20.90 kHz), for both on the left side to methanol and on the right side to 1-propanol.

In each plot of Fig. 6 two response modes are shown: the original sensor response on top and its first derivative (detector mode) below. An advantage of TSMRs is that the amount of the deposited coating can be determined from the frequency shift (Δf_{coat}) due to the added mass of the coating material. Two sensors with host compound **2c** were prepared, the first one with a thinner layer resulting in a Δf_{coat} value of approximately 9.87 kHz and the second one with a Δf_{coat} value of approximately 20.9 kHz (cf. Table 1). The actual values are given at the left ordinates. As can be seen from Fig. 6 the sensor signals of sensor **2c** (20.90 kHz) for methanol as well as for 1-propanol are approximately twice as high to those of sensor **2c** (9.87 kHz). Evidently, the absolute sensitivity ($\Delta f_{vap}/c$) increases linearly with Δf_{coat}, and the partition coefficient K_c can be calculated from the ratio of ($\Delta f_{vap}/c$) to Δf_{coat} as it is defined by equation 2. Therefore, K_c values represent a relative sensitivity *S*, so that the sensitivities of different kinds of coatings to a given vapour can be compared, standardised to unit coating mass. Sometimes numeric values of *S* differ from that of K_c due to the unit of the concentration in parts per million (*S*) instead of grams per liter (K_c).

Due to the increase of the Ostwald solubility coefficient (log L[16]) within the homologous series of the alcohols from methanol to 1-propanol and further by the decrease of their saturation vapour pressures, the sensor sensitivity expectedly increases in this order. Dependent on the coating thickness the equilibrium conditions and hence the steady state signal is not achieved within the given exposure period in all cases, as can be seen from sensor **2c** (20.9 kHz) in response to 1-propanol (Fig. 6). This effect can partly be compensated by reducing the coating layer thickness and extending the exposure periods respectively, as it is shown for sensor **2c** (9.87 kHz) to 1-propanol. In view of routine calibration the exposure periods were extended to the two- or fourfold for such host-vapour pairs which slow inclusion kinetics. However, for some coating-vapour pairs the sensitivities were estimated by signal extrapolation as described before.

On the other hand significant differences of the rate of inclusion formation facilitates a time dependent data recording. Hence the first derivative from the recorded frequency data was calculated and the signal heights were evaluated (detector mode). From the first derivatives in Fig. 6 can be seen that the order of sensitivity in the detector mode is inverse to that of the sensor mode. The positive peaks result from the sorption process, and the negative peaks results from the desorption process, respectively. In the detector mode only concentration changes are recordable but the drift of the baseline frequently observed with mass-sensitive transducers can be effectively minimized. For all tested host compounds **1** and **2** the signal height increases significantly with a decrease of the size of alcohol molecules. This effect can be improved when coating thickness increases. The signal height from the coating **2c** to methanol increases with the coating frequency of 9,87 kHz to 20,9 kHz, whereas the signal height to 1-propanol remains the same. Moreover, with decrease of the inclusion formation rate the half-width of the peak expands and an unsymmetrical peak shape is obtained, indicated by a typical tailing.

All investigated structures **1** and **2** exhibited the greatest inclusion rates with methanol, that produces a reversible sensor response as it is presented in Fig. 7. Here the response signal of host **1c** to methanol over a wide range from 200 ppm to 3800 ppm is shown.

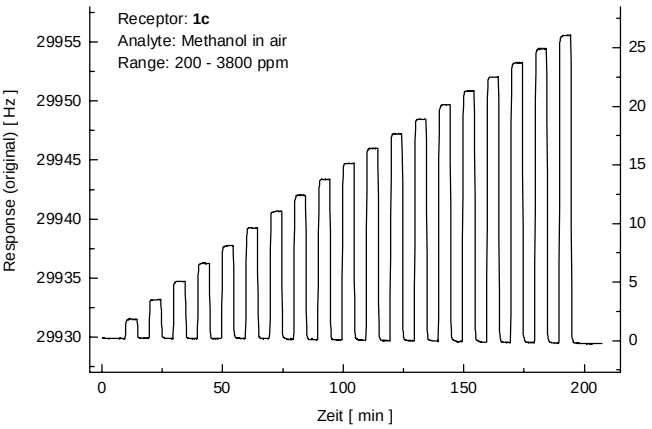

Fig. 7 Sensor response of 10 MHz TSMR coated with **1c** to methanol vapour in synthetic air, from (200, 400, ⋯ 3800) ppm $_{(V/V)}$ and (265, 530, ⋯ 5050) mg/m³, respectively. (A scanning electron image of the host topology of this sensor coating is given in Fig. 1).

The response and decay times (t_{90} and t'_{90}) vary in the range of minutes. The calibration curve is linear up to a vapour concentration of approximately one thousand parts per millions, accompanied by a slight decrease of the sensitivity with increasing concentrations. The sensitivity of water (humidity) is somewhat lower than that of methanol, in the sensor mode as well as in the detector mode. Except the diol host compound **2c** comprising the largest clathratogenic group (*tert*-butyl), the sensitivities of the hosts **1** and **2** to the other vapours are mostly lower than for the alcohols, which is discussed in detail as follows.

Sensitivity Patterns and Host Compound Structure

The present roof-shaped hosts **1** and **2** derive from a basic skeleton comprising of a 9,10-dihydro 9,10-ethanoanthracene framework. They differ by several appended clathratogenic groups as given in Scheme 1. For sensing purposes it is of prime interest if the clathrate formation ability can be controlled by different substitutents

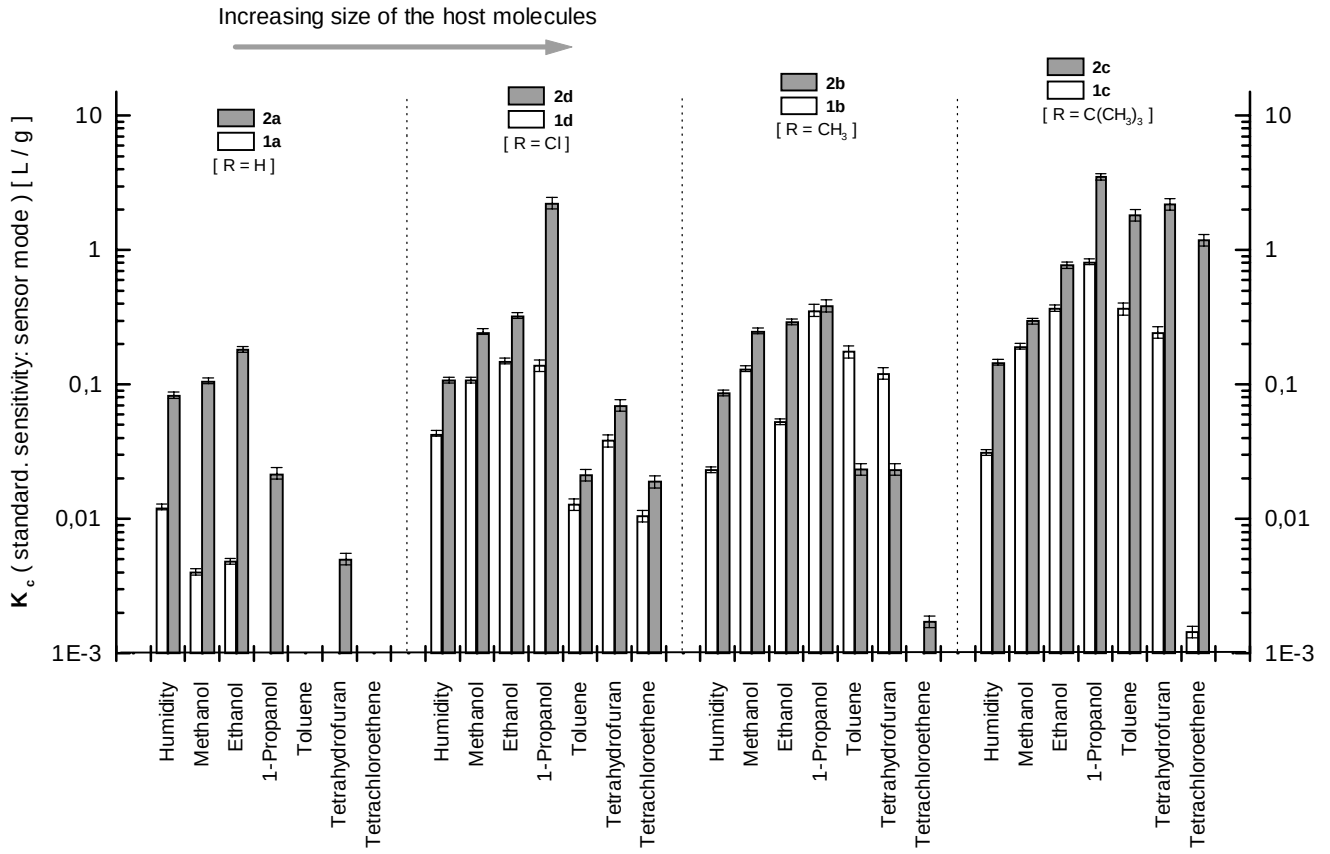

Fig. 8 Sensor sensitivity patterns of the sensor response expressed as K_c values according to the inclusion of host compounds **1a**–**d** and **2a**–**d** to selected organic solvent vapours and humidity.

Table 2 Survey of characteristic sensor values describing their performance. Calculation of the detection limit (LOD), the noise and drift level see before (Experimental Section)

Sensor (Δf_{coat})	Characteristics (sensor mode)	Analyte CH_3OH	C_2H_5OH	C_3H_7OH	H_2O
Qu 10-2c	S_{abs} ([Hz × ppm^{-1})	0,00826	0,03108	0,18363	0,00014
(20,90 kHz)	(R)	(0,99892)	(0,99940)	(0,99846)	(0,99802)
	LOD (ppm)	21,1	1,6	0,5	14,0
	Noise (Hz)	0,0175	0,0047	0,0085	0,0032
	Drift (Hz/h)]	0,193	0,091	0,332	0,494
Qu 10-1c	S_{abs} (Hz × ppm^{-1})	0,00667	0,00757	0,06107	0,00070
(29,95 kHz)	(R)	(0,99906)	(0,99997)	(0,99981)	(0,99998)
	LOD (ppm)	1,9	46,6	1,2	322,3
	Noise (Hz)	0,0013	0,0353	0,0073	0,0225
	Drift (Hz/h)	0,618	4,280	0,510	0,871
Qu 10-2b	S_{abs} (Hz × ppm^{-1})	0,01525	0,02794	0,04415	0,00295
(45,60 kHz)	(R)	(0,99913)	(0,99724)	(0,99975)	(0,99880)
	LOD (ppm)	9,7115	3,3822	1,9	24,0
	Noise (Hz =	0,01481	0,0095	0,0086	0,0071
	Drift (Hz/h)	1,498	1,804	0,069	1,020

thus finally improving the sensor selectivity. The complete sensitivity patterns of sensor measurements of coatings **1a**–**d** and **2a**–**d** to all vapours are given in Fig. 8.

Except the response of **1b** to toluene and tetrahydrofuran, the sensitivities of the monsubstituted hosts **1** are in all cases lower relative to the complementary compounds **2**, indicating that the bulky diol hosts **2a**–**d** show substantial improvements over the hosts of type **1a**–**d**. The second effect is given by the substituents. The size of the host compound increases from the left to the right due to the appended groups as it is shown in the graph. In this order we found a permanent increase of the sensor sensitivity, for hosts of type **1** as well as for hosts **2**. So the bulky diol host **2c** shows the highest sensitivities to all examined vapours comparable to those of poly-

mer rubbers often used as sensitive coatings [4, 5]. With a decrease in the host size the sensitivity pattern shifts to molecules with smaller molar volume, preferably alcohol molecules and humidity are enclathrated. In particular the pore sizes of **1a** and **2a** are small enough to exclude large molecules efficiently, but the absolute sensitivity is rather small.

In this context, the obtained host size dependent sensitivity patterns raise the question, whether this effect can be denoted as molecular recognition. In summary, three major effects seem to be predominant: the hydrogen bond interaction between the present roof-shaped hosts **1** or **2** and guests exhibiting proton donor and/or acceptor abilities (humidity, alcohols, tetrahydrofuran), which agrees very well to systematic X-ray investigations of **1a**–**d** [25] and **2a**–**d** [25, 27, 30]. Secondly, the appended groups of a host seem to create variable pore sizes and, therefore, guest molecules are included or excluded according to size. And finally, the solubility characteristics of the analyte molecules, usually expressed as their Ostwald solubility coefficients (log L[16]), lead to a continuous increase of the clathrate formation for lipophilic molecules such as toluene or tetrachloroethene with increasing size of the host. For a brief estimation of the selected sensor performance some characteristic values are summarised in Table 2.

The good quality of the measuring device is indicated by the excellent noise levels, which are given as the average standard deviations from approx. 100 discrete data points of the baselines. Therefore, low detection limits were calculated (see Experimental Section), which can hardly be achieved in practical use. Furthermore, such stabilities of the noise and the baseline were mainly obtained for the alcohols and humidity. For other vapours studied or for host–guest pairs with low sensitivities, the stabilities of electronic and chemical noise and the baseline drift near the detection limit were not so optimal as for alcohols.

Relating to the preferred interaction to alcohol guests, in particular methanol, a significant improvement of the signal selectivity was obtained by the analysis of the peak height of the first derivative of the sensor signal, as described above in detail (Fig. 6). The complete sensitivity patterns from the measurements in the detector mode of coatings **1a**–**d** and **2a**–**d** to all vapours are given in Fig. 9.

All examined hosts **1** and **2** show pronounced selectivity to methanol, thus indicating high inclusion formation rates in the presence of methanol molecules, resulting in a peak height ratio of methanol to ethanol, *e.g.* for **2b** of approximately 35 : 1. With this recording technique the major influence of solubility effects to the sensor signal was reduced efficiently, even within the homologous series of the alcohols. Moreover, it was possible to minimize the cross sensitivity to humidity, which should be as low as possible for practical applications. Conclusions made from sensitivity patterns in the sensor mode (cf. Fig. 8) with respect to the analytes

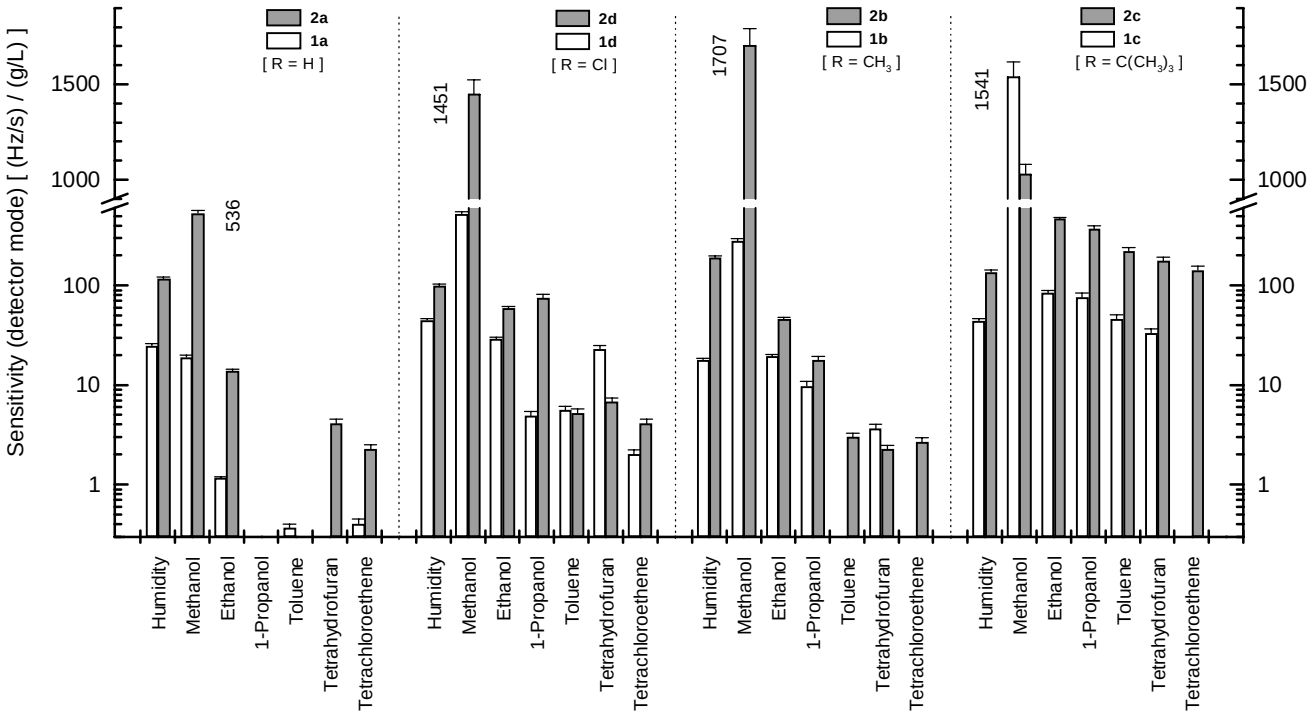

Fig. 9 Sensitivity patterns of the signal height from the first derivative of the frequency sensor signals of the host compounds **1a**–**d** and **2a**–**d** to selected organic solvent vapours and humidity.

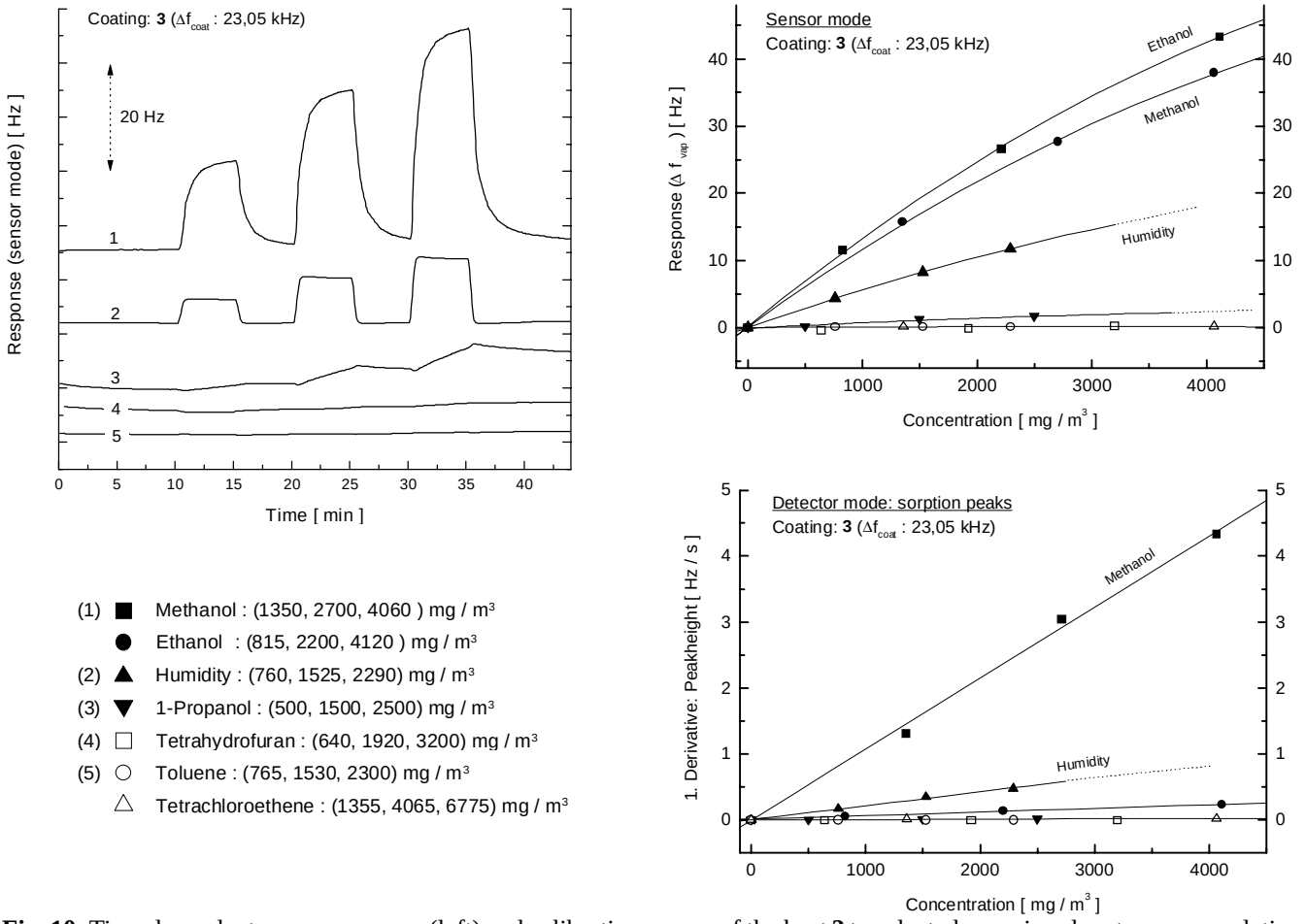

Fig. 10 Time dependent sensor response (left) and calibration curves of the host **3** to selected organic solvent vapours, relating to the sensor mode (above) and the detector mode (below).

and host size agree with obtained results in the detector mode (Fig. 9).

Sensitivity and selectivity

As shown in Figs. 8 and 9, systematic sensor studies of synthetic host molecules provide excellent opportunities for an investigation of host–guest interactions, with the aim to obtain sensing receptors for selected target molecules showing high sensitivity as well as high selectivity. The racemic host compound **3** nearly meets the necessary requirements and is described separately (Fig. 10).

In conformance with the results of inclusion formation experiments by cocrystallisation, where host **3** formed numerous inclusion compounds with alcohols of different size and shape [26, 28], we found preferred sensitivity to methanol and ethanol. Surprisingly, the sensitivity to 1-propanol was somewhat lower. Selected time dependent sensor responses from those calibrations with identical exposure–purging periods are summarised in Fig. 10 (left). The corresponding sensor calibration curves including all vapours is shown in the top graph. In contrast to the hosts **1** and **2**, here a total exclusion of other molecules than methanol, ethanol and, to some extend, humidity, was observed. Even high lipophilic guest molecules such as toluene or tetrachloroethene do not show significant interaction to the host compound **3**. As described above, due to the high vapour permeability of methanol in host **3** high selectivity to methanol can be obtained when the signal height of the sorption peaks is analyzed (Fig. 8, right, bottom). The improvement of methanol selectivity from sensor mode to detector mode is separately shown in figure 11 including specification of the Ostwald solubility coefficients (log L^{16}) and vapour pressures at 1 013 hPa and 293.15 K.

As evident from this figure, solvents having high log L^{16} values and/or low vapour pressures do not exhibit appreciable interaction to host compound **3**. Obviously, the influence of the solid structure is such strong that big differences in the permeability are between the small alcohol molecules (and humidity) and the other solvent molecules. Including the distinct activity of compound **3** to form hydrogen bonds, the object of molecular recognition by using a designed host is near at the hand.

Sensor Age and Coating Stability

The lifetime of a receptor based sensor is usually determined by the stability of its coating layer. Here the quartz microbalance, in particular the TSMR, is an ideal instrument to control the mass stability of the deposited material over a wide period. It can be assumed that sensing abilities remain constant provided that the coating mass is stable. To investigate the mass stability of the present hosts **1**–**3** the Δf_{coat} values of the TSMRs were measured regular over a period of more than two years. Measurements were done in ambient laboratory atmosphere. So the Δf_{coat} values are slightly higher (1–2% on average) than these from Table 1. In addition, Δf_{coat} values can vary due to fluctuations of room temperature or ambient humidity. The results are presented as the deviations to each mean value ($\Delta f_{coat,\,mean}$) including the standard deviation given at the bottom of the bar chart (Fig. 12).

In summary, all deposited hosts show very small deviations from the mean value and therefore excellent mass stability. Some coatings such as **2a**, **2b** and **3** exhibit a minimal systematic decrease of Δf_{coat} values, whereas Δf_{coat} of the other coatings show only random fluctuations.

Conclusions

In this contribution a systematic study on a series of roof-shaped crystalline host compounds as coating materials onto TSMRs is presented, referring to their sensing abilities for the detection of selected organic solvent vapours. From the obtained sensitivity patterns to each of seven individual organic solvent vapours we conclude that host–guest interactions are predominantly given by hydrogen bonds, resulting in a preferred sensitivity to alcohols and humidity, which is in good agreement with results from systematic x-ray studies [25–28, 30]. Within the homologous series of the alcohols, the sensitivity patterns from hosts **1a**–**d** and **2a**–**d** increase from methanol to 1-propanol, which is accompanied by a general increase of the sensitivity with increasing size of the hosts. Improved sensor selectivity for methanol and ethanol was found for the host compound **3**, even toward high lipophilic molecules such as toluene or tetrachloroethene. For all host compounds under study we observed significant differences with respect to the inclusion rate behaving inversely to the equilibrium sensor signal. By time dependent data acquisition and the analysis of the signal height of the peaks due to the sorption process a selectivity to meth-

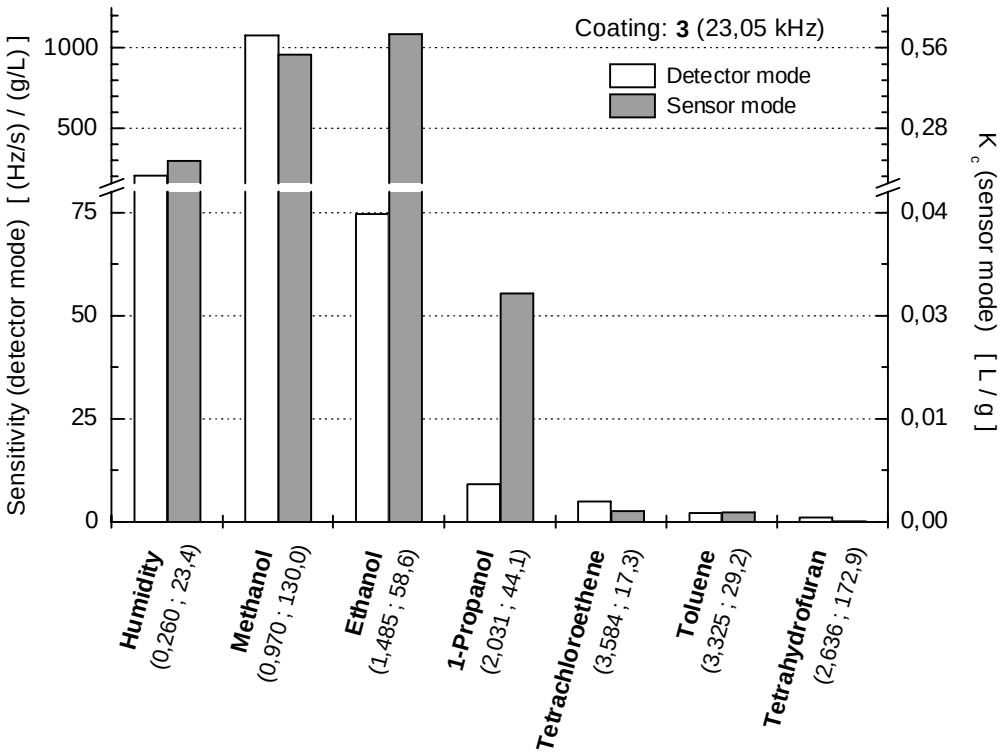

Fig. 11 Improvement of the selectivity of the host **3** to alcohols from the sensor mode to the detector mode. In the detector mode the signal height of the sorption peaks resulting from the first derivative of the sensor signal was analyzed. (In parentheses: Ostwald solubility coefficients log L[16]; vapour pressure at 1 013 hPa and 293.15 K).

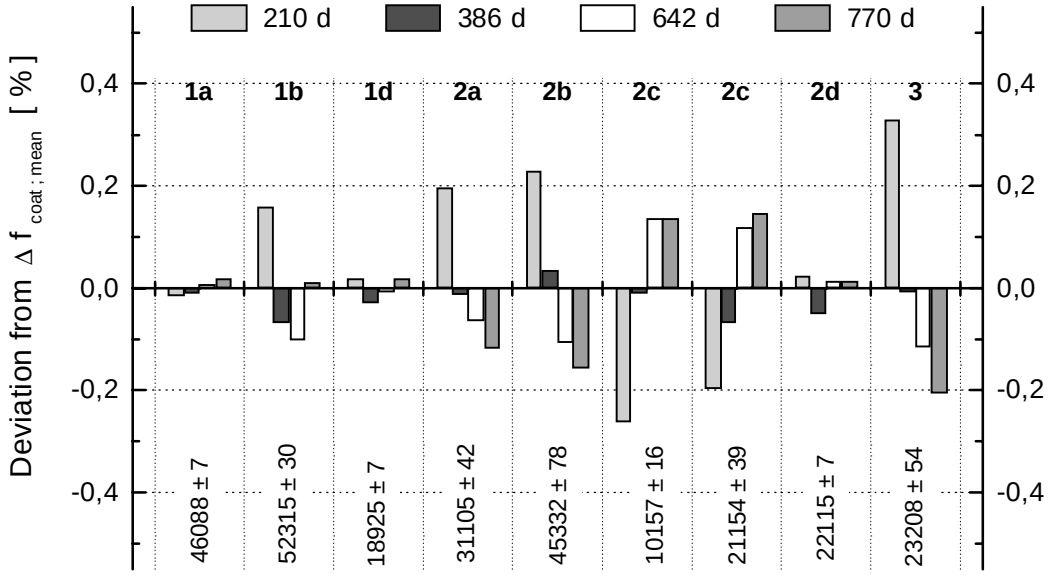

Fig. 12 Mass stability of sensor coatings **1a**, **1b**, **1d**, **2a**–**d** and **3** relating to measurements of Δf_{coat} [Hz] over a period of more than two years. The ambient temperatures at the measuring dates were 21.3 °C (210. day), 21.0 °C (386. day), 20.9 °C (642. day) and 22.0 °C (770. day), each with a deviation of approx. ± 0,1 °C.

anol is evident. Especially the hosts **2b**, **2d** and **3** have shown excellent methanol over ethanol selectivity, indicated by 20–35 fold signal heights relative to ethanol. Although it is true that results obtained from gas-solid interface are no real evidence that justifying the term "molecular recognition", the present approach is promising to obtain designed materials featuring definite selectivities.

References

[1] J. Janata, M. Josowicz, P. Vanysek, M.D. DeVaney, Anal. Chem. **1998**, *70*, 179R
[2] J. Reinbold, K. Cammann, GIT **1998**, *4*, 396
[3] W. Göpel, Sensors and Actuators B **1995**, *24*, 17
[4] R. A. McGill, M. H. Abraham, J. W. Grate, Chemtech **1994**, *24*, 27
[5] J. W. Grate, M. H. Abraham, R. A. McGill, in Handbook of Biosensors and Electronic Noses: Medicine, Food, and the Environment, (E. Kress-Rogers ed.), CRC Press Inc., Boca Raton 1997, chapter 25
[6] M. Reif, F. L. Dickert, H. Reif, Fresenius J Anal Chem **1995**, *352*, 620
[7] F. L. Dickert, A. Haunschild, V. Maune, Sensors and Actuators B **1993**, *12*, 169
[8] F. L. Dickert, A. Haunschild, M. Reif, W.-E. Bulst, Adv. Mater. **1993**, *5*, 277
[9] F. L. Dickert, O. Schuster, Adv. Mater. **1993**, *11*, 826
[10] A. Ehlen, C. Wimmer, E. Weber, J. Bargon, Angew. Chem. **1993**, *105*, 116
[11] K. Buhlmann, J. Reinbold, K. Cammann, K. Skobridis, A. Wierig, E. Weber, Fresenius J Anal Chem **1994**, *348*, 549
[12] J. Reinbold, K. Buhlmann, K. Cammann, A. Wierig, C. Wimmer, E. Weber, Sensors and Actuators B **1994**, *18*, 77
[13] T. Weiss, J. Rickert, W. Göpel, Sensors and Actuators B **1996**, *31*, 45
[14] F. L. Dickert, M. E. Zenkel, W.-E. Bulst, G. Fischerauer, U. Knauer, Fresenius J Anal Chem **1997**, *357*, 27
[15] M. S. Nieuwenhuizen, A. W. Barendsz, Sensors and Actuators **1987**, *11*, 45
[16] J. C. Brice, Reviews of Modern Physics **1985**, *57*, 105
[17] Hy-Q Handbook of Quartz Crystals Devices, D. Salt, Van Nostrand Reinhold (UK), Wokingham, Berkshire 1987
[18] B. Neubig, UKW-Berichte **1979**, *1*, 45
[19] G. Sauerbrey, Z. Physik **1959**, *155*, 206
[20] C. Lu, in Methods and Phenomena 7: Applications of Piezoelectric Quartz Crystal Microbalances (C. Lu, A. W. Czanderna, eds.), Elsevier, Amsterdam 1984, chapter 2
[21] J. W. Grate, S. J. Patrash, M. H. Abraham, Anal. Chem. **1995**, *67*, 2162
[22] S. J. Patrash, E. T. Zellers, Anal. Chem. **1993**, *65*, 2055
[23] J. W. Grate, M. H. Abraham, C. My Du, R. A. McGill, W. J. Shuley, Langmuir **1995**, *11*, 2125
[24] J. W. Grate, S. J. Patrash, M. H. Abraham, Anal. Chem. **1996**, *68*, 913
[25] E. Weber, T. Hens, O. Gallardo, I. Csöregh, J. Chem. Soc., Perkin Trans. **1996**, *2*, 737
[26] E. Weber, C. Reutel, C. Foces-Foces, A. L. Lamans-Saiz, J. Chem. Soc., Perkin Trans. **1994**, *2*, 1455
[27] I. Csöregh, E. Weber, T. Hens, M. Czugler, J. Chem. Soc., Perkin Trans. **1996**, *2*, 2733
[28] E. Weber, C. Reutel, C. Foces-Foces, A. L. Llamas-Saiz, J. Phys. Org. Chem. **1995**, *8*, 159
[29] VDI Richtlinie 3490, Blatt 13, VDI-Verlag, Düsseldorf 1980
[30] I. Csöregh, E. Weber, in: Molecular Recognition and Inclusion (A. W. Coleman, ed.), Kluwer, Dordrecht 1998

Address for correspondence:
Prof. Dr. K. Cammann
Anorganisch-Chemisches Institut, Lehrstuhl für Analytische Chemie
Westfälische Wilhelms-Universität Münster
Wilhelm-Klemm-Str. 8
D-48149 Münster
Fax: Internat. code (0)251 980 2802
e-mail: cammann@uni-muenster.de